Suppression of electroconvection by Couette shear in freely suspended smectic C* films

C. Langer[a], Z. A. Daya[b,c], S. W. Morris[b], R. Stannarius[a]

[a] *Universität Leipzig, Linnéstrasse 5, 04103 Leipzig, Germany*

[b] *University of Toronto, Department of Physics,*

60 St. George St., Toronto, Ontario, Canada, M5S 1A7

[c] *Center for Nonlinear Studies, MS-B258, Los Alamos National Laboratory,*

Los Alamos, New Mexico 87545

We present the first experiments on electrohydrodynamic convection with a superposed Couette shear in freely suspended annular smectic C^* films. Similar experiments on smectic A films have been carried out previously. In those experiments, surface-charge driven electroconvection in combination with shear leads to a pattern of travelling convective vortices. Travelling vortex patterns are also observed in smectic C^* films. In contrast to smectic A films, however, the flow field in C^* films is coupled to c-director orientation effects that allow a direct visualization of the periodic flow pattern. The critical voltage for the onset of convection was determined by electric current measurements and compared with corresponding results for smectic A films. Measurements at various shear rates show that the onset is suppressed by the shear.

Submitted to *Molecular Crystals and Liquid Crystals*, August 2000.

INTRODUCTION

Freely suspended smectic liquid crystal films provide a suitable geometry for the investigation of two-dimensional electrooptical and electrohydrodynamical processes. One of the most impressive phenomena that can be studied in such systems is the formation of electrohydrodynamic convection patterns. When a sufficiently high electric field is applied in the plane of the smectic layers, a quasi-two-dimensional periodic flow is observed which consists of counter-rotating vortices. Electroconvection in rectangular smectic A films has been intensively studied both theoretically and experimentally [1–6]. Recently, annular smectic A films have also been investigated [7,8]. In such films, one can observe the interaction of convective instabilities with a separately imposed azimuthal Couette shear.

While the theoretical description for electroconvection in smectic A films is well established and in good agreement with experimental results, electrohydrodynamic instabilities in smectic C^* films are less well understood. Previous investigations in a rectangular geometry suggested that two mechanisms might be responsible for the formation of convective vortices. In addition to the surface charge mechanism described by Daya et al. [5,6] that does not depend on the specific LC phase, an anisotropic mechanism similar to the well-known nematic Carr-Helfrich effect has also been theoretically considered [9] and experimentally observed [11,12]. It seems likely that a generalized theory, taking into account both charge generation mechanisms, would be necessary to describe electroconvection in smectic C^* films.

Our experimental apparatus is the same as used previously in the experiments on smectic A films described in Ref. [8]. A schematic sketch of the annulus is shown in Figure 1. It is formed by two thin concentric circular electrodes made of stainless steel with a thickness of $0.73 \pm 0.01\,mm$. The inner electrode is a disk with a diameter of $2r_i = 1.05 \pm 0.001\,cm$, while the outer electrode is a fixed disk that has a circular hole with diameter $2r_o = 1.31 \pm 0.001\,cm$. Together, they form an annulus with a radius ratio $\alpha = r_i/r_o = 0.80$. The inner electrode can be rotated around its axis by a stepper motor at angular frequencies up to $6.3\,\mathrm{rad/s}$. In order to provide electric shielding, the whole electrode system was enclosed in a grounded

aluminum box. For some runs, the box was evacuated to eliminate air drag on the film. The liquid crystal mixture FELIX 016-100 is used which has a S_C^* phase below $72°C$. The experiments were performed at room temperature $T = 23 \pm 1°C$. Freely suspended films are prepared by using a razor blade wetted with liquid crystal material which is slowly drawn over the annular film holder. When a voltage is applied between the inner and outer electrode, the film is driven by a radial electric field. Above a certain threshold voltage U_C, electroconvective flow sets in [7,8]. The film can also be subjected to a Couette shear by rotating the inner electrode. The shear leads to a net mean flow in the azimuthal direction and breaks the symmetry of the unconvecting base state. Unlike three-dimensional Couette flow, which is unstable to the formation of Taylor vortices, 2D Couette flow without applied voltage is absolutely stable. Our protocol was always to establish the Couette shear before examining its stability by slowly increasing and decreasing the applied voltage. As described in [8], the steady shear always has the effect of suppressing electroconvection; the sheared base state is more stable than the unsheared state. On the other hand, the shear significantly changes the flow pattern to one which consists of asymmetric, travelling vortex pairs. The vortices rotating in the sense of rotation of the inner electrode become narrower, while their counter-rotating neighbours become broader.

EXPERIMENTS

In the smectic A phase, which is isotropic in the layer plane, the flow field can be visualized only by test particles or moving regions of non-uniform film thickness [2]. In the smectic C and C^* phases, the flow is coupled with birefringent effects due to the anisotropy in the layer plane [10,11]. The orientation of the c-director interacts with the applied electric field via the dielectric anisotropy. In smectic C^*, there is an additional strong coupling to the spontaneous polarization $\vec{\mathbf{P}}_s$, which lies in the plane of the layers. The c-director also reorients under hydrodynamic torques within each vortex and therefore varies locally. This non-uniform c-director field can be resolved by polarizing microscopy. In electroconvecting

smectic C^* films, the strong coupling to $\vec{\mathbf{P}}_s$ constrains the c-director field so that it is deflected in the direction of the rotational flow by rather small deflection angles between zero and 20° (see [11] for a detailed description). When the polarizers are crossed and the polarizer orientation is not aligned with the c-director, vortices with opposite senses of rotation are characterized by different brightness in reflected light. This effect can also be observed for electroconvection with azimuthal shear in the annulus. In order to visualize the flow field, the annular film was observed in reflected light with a simple lens system that included a polarizer and an analyzer, providing magnifications between 5x and 15x. Although the accuracy of this optical setup was lower than that of a standard polarizing microscope, the reflected intensity of some thicker films ($s \geq 200nm$) was high enough to obtain sufficient contrast between images of neighbouring vortices. Fig. 2 shows an image of a section of the annulus obtained in this way. The main features of the flow pattern could be reproduced on the images recorded with a CCD camera and a VCR. In principle, the periodicity of the flow field, the size of the asymmetric vortices and their travelling speed can be measured. This visualization method provides a more convenient alternative to the tracer particle measurements reported in [2] and [11,12], since it does not introduce any additional impurities or pertubations but rather gives direct insight into the structure of both the flow field and the c-director orientation.

Electric current measurements were used to determine the critical voltage U_C for the onset of convection. The current I through the annular film was measured as a function of the voltage applied, which was increased in small steps from zero to sufficiently high voltages above the onset. During such a run, the shear rate was kept constant. For the current measurements, a high precision Keithley Electrometer was used that allows for the detection of small currents in the subpicoampère range. As reported in [2] and [8], the onset of convection appears as a kink in the I-U-curve, separating the linear ohmic conduction from the non-Ohmic range. An example is shown in Figure 3. Below the critical voltage U_C, the film behaves as a weak ohmic conductor with the linear relation $I = cU$. The

conductance c of the annular film is given by

$$c = \frac{2\pi\sigma s}{ln(1/\alpha)}. \tag{1}$$

where s is the film thickness and σ the conductivity in the direction of the applied electric field. Above U_C, conductive and convective current both contribute to the overall electric current and the I-U-curve becomes nonlinear. However, this method for the detection of the onset of convection works properly only in case of films with uniform thickness. If there are regions of non-uniform thickness, the curve becomes irregular and the onset can not be clearly detected. Our experiments have shown that such thickness inhomogenities can easily form even for uniform films if the film has a thick meniscus at the electrode edges with excess liquid crystal material that might be advected with the convective flow. Therefore, the preparation of the films has to be carried out very carefully in order to minimize the deposition of smectic material at the edges.

We recorded I-U curves at various shear rates for several films. As expected, the shear shifts the critical voltage to higher values. These results may be compared with corresponding data for smectic A films. For that purpose, the same dimensionless quantities as given in [8] are introduced: The relative suppression of the onset voltage is defined as

$$\tilde{\epsilon}(Re) = \left[\frac{R_c(Re)}{R_c(Re=0)}\right] - 1 = \left[\frac{U_c(Re)}{U_c(Re=0)}\right]^2 - 1. \tag{2}$$

For purely surface-charge-driven convection, the critical value of the Rayleigh-like dimensionless parameter R is given by

$$R_c = \frac{\epsilon_0^2 U_c^2}{\sigma\,\eta s^2}. \tag{3}$$

For more complex charge generation mechanisms, dimensional analysis suggests that the scaling $R_c \sim U_c^2$ will still be correct. The second essential scaling parameter in the stability analysis for electroconvection is the Prandtl number

$$Pr = \frac{\epsilon_0\,\eta}{\rho\,\sigma\,(r_o - r_i)\,s}. \tag{4}$$

The Reynolds number Re is given by

$$Re = \frac{\rho\,\omega\,r_i(r_o - r_i)}{\eta}. \tag{5}$$

The conductivity σ and the shear viscosity η can be determined from the zero shear electroconvection experiments via equations 1 and 3 as described in [8]. We obtained an average conductivity value of $\sigma = 5 \cdot 10^{-9}(\Omega m)^{-1}$ which is in reasonable agreement with results from dielectric measurements with the same smectic mixture FELIX 016-100. The value for the shear viscosity obtained from a fit to the experimental data was $\eta = 0.37 \pm 0.05\,kg\,(m\,s)^{-1}$. This is about a factor of 2 higher than that for 8CB reported in [8], but within the expected range for this smectic C^* material which is more viscous at room temperature than 8CB. The density ρ of the liquid crystal material is assumed to be $10^3 kg\,m^{-3}$. The film thickness was independently determined by a colorimetric method [8,13].

The relative suppression $\tilde{\epsilon}(Re)$ shows an approximately linear increase with Re within the experimental error, similar to the smectic A experiments (Figure). On the other hand, we note that the suppression values are obviously higher than those reported by Daya et al. [7,8] for similar Reynolds numbers. For example, we obtained $\tilde{\epsilon}(Re) = 62$ for $Re = 0.086$, which shows very impressively how much the shear stabilizes the base state against electroconvective instabilities. A direct comparison to the smectic A experiments is difficult since for our smectic C^* films, the Prandtl numbers were at least one order of magnitude higher than in Refs. [7,8]. For the experimental data shown in in Figure , we estimated a Prandtl number of 2160, while in Ref. [8] the maximum value for Pr was 100. However, we can compare our data with the theoretical predictions for the relative suppression of the onset in smectic A films with $Pr = 2160$.

Figure shows the results of the calculation, which are of the same order of magnitude as our experimental data, but systematically lower. Some of this discrepancy could be accounted for by air-drag effects, which are not included in the theory. Another difference from the smectic A measurements is that no hysteretic jumps have been observed in the I-U curves. Such discontinuities, which indicate subcritical bifurcations, were reported in

Ref. [7] for sufficiently high shear rates. It could be that the Reynolds numbers for our measurements (which were carried out at atmospheric pressure) were not high enough to observe this effect.

In addition to the shear experiments described above, various electroconvection measurements on smectic C^* films without shear have been carried out in the annulus which might be compared to previous experiments in a rectangular geometry [11,12]. We found a clear and puzzling discrepancy between the experimental results obtained in these two different setups: In the rectangular geometry, a very low onset voltage for convection was taken to indicate that an anisotropic charge generation mechanism, similar to Carr-Helfrich, was operating close to onset, while surface-charge driven convection seems to be not more than a secondary effect at higher electric fields [12]. On the other hand, our observations in the annular geometry strongly indicate a surface charge mechanism. The onset voltages, located with the current-voltage measurements, are consistent with a surface charge mechanism and show the expected linear dependence on the film thickness. Although the existence of an anisotropic mechanism in the annulus cannot be definetely excluded, no evidence for such a mechanism has been found.

DISCUSSION

The differing results of the non-shear experiments reported above might be explained by a geometry-dependent cross-over between the two mechanisms: While the surface charge mechanism dominates in the limit of very thin films ($s \ll d$) and with flat plate electrodes where the geometry is well approximated by the two-dimensional model described by Daya et al., the anisotropic mechanism would be favoured in a three-dimensional geometry. The critical field for the onset of anisotropic electroconvection was experimentally found to be of the order of $10^4 V/m$, without significant film thickness dependence. For the annulus described above, this corresponds to an expected critical voltage $U_c \geq 10V$. However, the onset voltages determined from current measurements in unsheared films with thicknesses

$s \leq 250nm$ were all lower than $10V$ and were a decreasing function of the film thickness. Since these values are also quanitatively in reasonable agreement with the predictions of the theory described in [8], we hypothesize that in the thin smectic C^* films investigated, the onset voltage of surface charge electroconvection is lower than the onset voltage for the anisotropic mechanism. This situation would reverse with increasing film thickness s and decreasing electrode distance d: The critical voltage of the surface charge mechanism is shifted to higher voltages with increasing s, whereas the onset voltage for anisotropic convection decreases with d due to the constant critical field $E_c = U_c/d$. Thus, in thick films with low electrode distances as used in the experiments described in [12], the anisotropic mechanism has the lower threshold. In principle, the crossover between the two mechanisms could be observed by varying the dimensionless ratio s/d, which controls the relative size of the forcing terms in the Navier Stokes equation [5]. We were not able to observe this crossover in the present experiments.

CONCLUSION

We have presented the first electroconvection experiments on annular smectic C^* films with and without a superposed shear. In such films, one can exploit the director reorientation effects to directly observe the travelling flow pattern under shear. The critical voltage for the onset of convection was determined from electric current measurements. Different zero-shear results obtained in rectangular and annular geometry might be interpreted by a geometry dependent cross-over between two different convection mechanisms. In experiments with azimuthally applied Couette shear, the onset of convection is suppressed. The relative suppression is comparable to corresponding results for smectic A films and in fair agreement with theoretical predictions.

Acknowledgements

This research was supported in part by the German Academic Exchange Service (DAAD), the Natural Science and Engineering Research Council of Canada and the Department of Energy, under contract W-7405-ENG-36.

---

[1] S. W. Morris, J. R. de Bruyn, A. D. May; *Phys. Rev. Lett.* **65**, 2378 (1990).

[2] S. W. Morris, J. R. de Bruyn, A. D. May; *Phys. Rev. A* **44**, 8146 (1991).

[3] S. S. Mao, J. R. de Bruyn, Z. A. Daya, S. W. Morris; *Phys. Rev. E*, **54**, R1048 (1996).

[4] S. S. Mao, J. R. de Bruyn, S. W. Morris; *Physica A*, **239** 189 (1997).

[5] Z. A. Daya, S. W. Morris, J. R. de Bruyn; *Phys. Rev. E.* **55**, 2682 (1997).

[6] V. B. Deyirmenjian, Z. A. Daya, S. W. Morris; *Phys. Rev. E* **56** 1706 (1997).

[7] Z. A. Daya, V. B. Deyirmenjan, S. W. Morris, J. R. de Bruyn; *Phys. Rev. Lett.* **80**, 964 (1998).

[8] Z. A. Daya, V. B. Deyirmenjian, S. W. Morris; *Physics of Fluids* **11**, 3613 (1999).

[9] S. Ried, H. Pleiner, W. Zimmermann, H. R. Brand; *Phys. Rev. E* **53**, 6101 (1996).

[10] A. Becker, S. Ried, R. Stannarius, H. Stegemeyer, *Europhys. Lett.* **39**, 257 (1997).

[11] C. Langer, R. Stannarius; *Phys. Rev. E.*, **58**, 650 (1998).

[12] C. Langer, R. Stannarius; *Mol. Cryst. Liq. Cryst.* **328**, 533 (1999).

[13] E. B. Sirota, P. S. Pershan, L. B. Sorenson and J. Collett; *Phys. Rev. A* **36**, 2890 (1987).

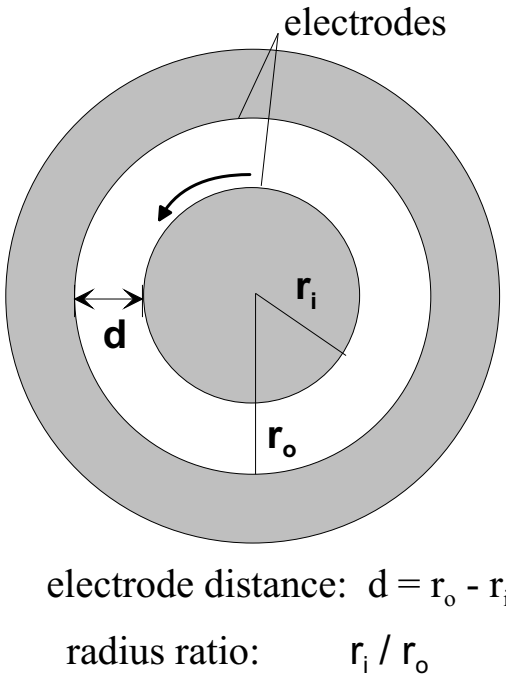

FIG. 1. Schematic sketch of the frame used for electroconvection and shear experiments in smectic C^* films. The annulus is formed by a disk with a circular concentric hole of radius r_o and an inner disk with radius r_i that can be rotated around its axis. Both disks serve as electrodes.

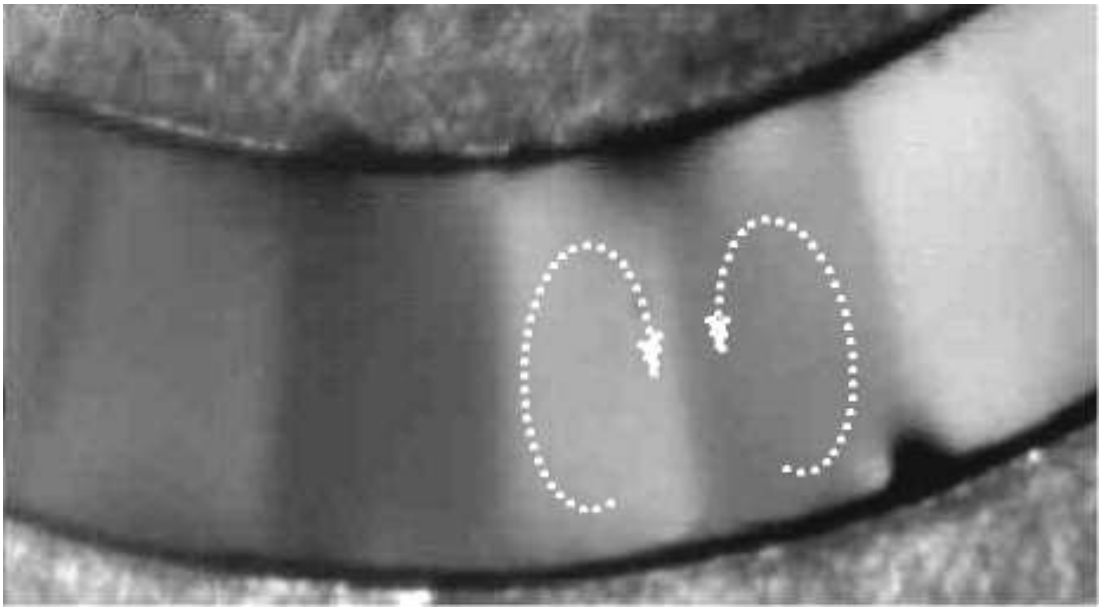

FIG. 2. A photo of the convective flow pattern in a smectic * film in reflected white light with crossed polarizers. Dashed lines indicate the direction of the vortex flow. The reversing tilt orientation of the c-director in adjacent vortices is visible.

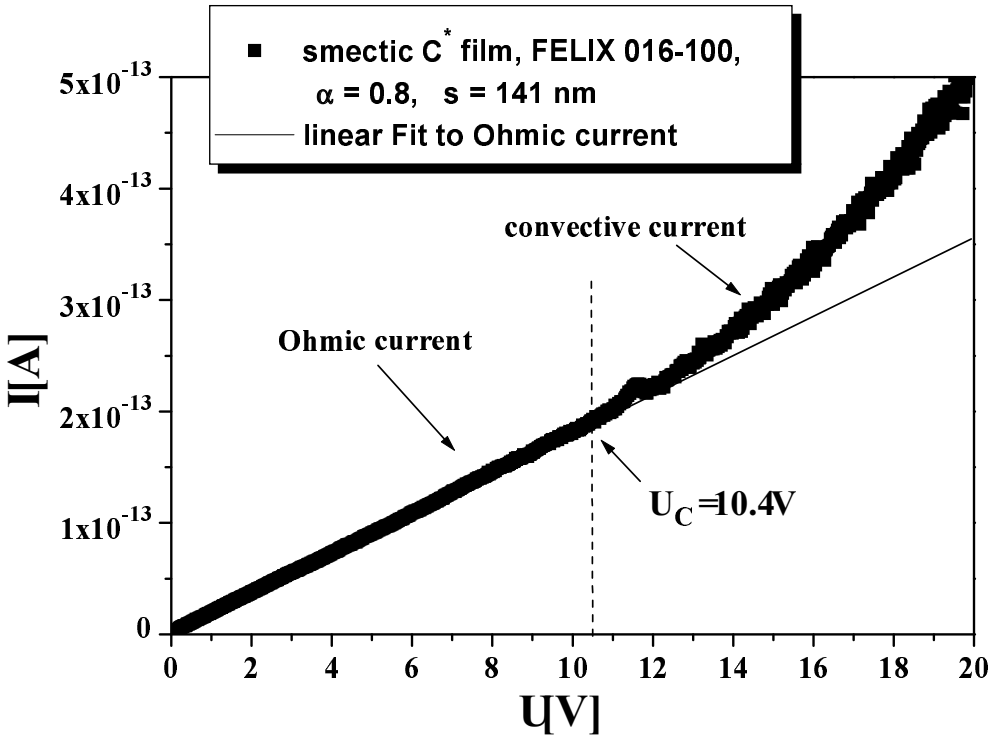

FIG. 3. Onset of electroconvection detected by current measurements for a thin annular smectic C^*-film (FELIX 016-100, $s = 141nm$, $\alpha = 0.8$,) sheared with a frequency of $\omega = 0.314 rad/s$. Below the critical voltage U_C, the film behaves as a weak Ohmic conductor.

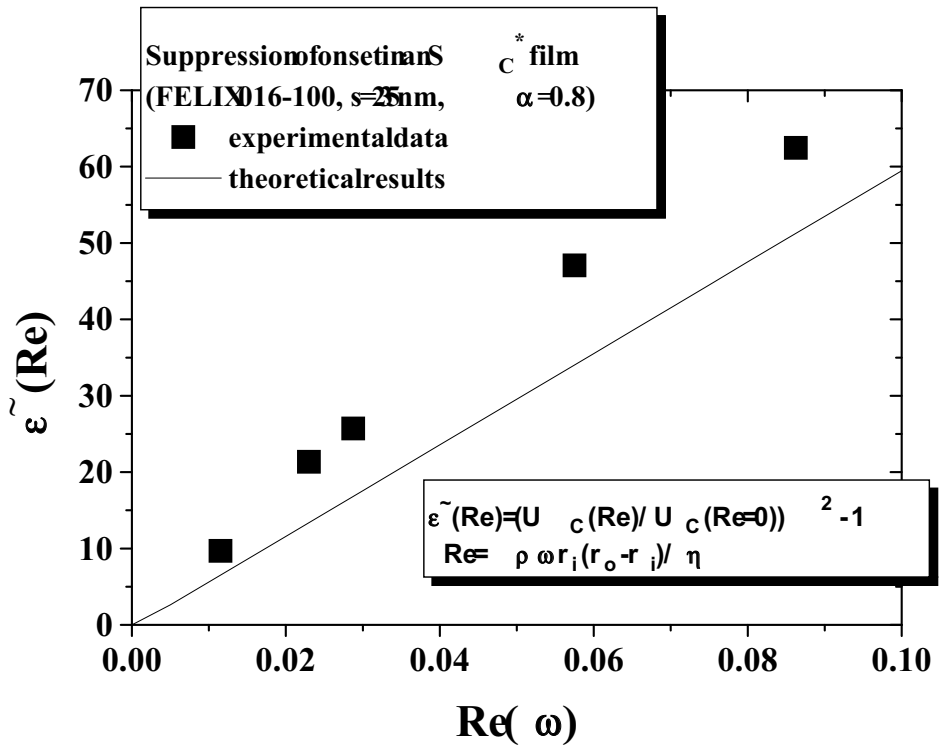

FIG. 4. Relative suppression of the onset of electroconvection in a smectic annular smectic C^* film (FELIX 016-100, $\alpha = 0.8$, thickness: $s = 235nm$) as a function of the Reynolds number Re. The measurements were performed at atmospheric pressure.